Letter

Phonon renormalization effects accompanying the 6 K anomaly in the quantum spin liquid candidate κ-(BEDT-TTF)$_2$Cu$_2$(CN)$_3$

Masato Matsuura,[1,*] Takahiko Sasaki,[2] Makoto Naka,[3] Jens Müller,[4] Oliver Stockert,[5] Andrea Piovano,[6] Naoki Yoneyama,[7] and Michael Lang[4]

[1]*Neutron Science and Technology Center, Comprehensive Research Organization for Science and Society (CROSS), Tokai, Ibaraki 319-1106, Japan*

[2]*Institute for Materials Research, Tohoku University, Sendai 980-8577, Japan*

[3]*School of Science and Engineering, Tokyo Denki University, Saitama 350-0394, Japan*

[4]*Institute of Physics, Goethe-University Frankfurt, 60438 Frankfurt (M), Germany*

[5]*Max-Planck-Institut für Chemische Physik fester Stoffe, D-01187 Dresden, Germany*

[6]*Institut Laue-Langevin (ILL), 71 avenue des martyrs, 38042 Grenoble Cedex 9, France*

[7]*Graduate Faculty of Interdisciplinary Research, University of Yamanashi, Kofu 400-8511, Japan*

(Received 8 August 2022; accepted 23 November 2022; published 20 December 2022)

The low-temperature state of the quantum spin liquid candidate κ-(BEDT-TTF)$_2$Cu$_2$(CN)$_3$ emerges via an anomaly at $T^* \sim 6$ K. Although signatures of this anomaly have been revealed in various quantities, its origin has remained unclear. Here we report inelastic neutron scattering measurements on single crystals of κ-(BEDT-TTF)$_2$Cu$_2$(CN)$_3$, aiming at studying phonon renormalization effects at T^*. A drastic change was observed in the phonon damping across T^* for a breathing mode of BEDT-TTF dimers at $E = 4.7$ meV. The abrupt change in the phonon damping is attributed to a phase transition into a valence bond solid state based on an effective model describing the spin-charge coupling in this dimer-Mott system.

DOI: 10.1103/PhysRevResearch.4.L042047

Quantum spin liquids (QSLs) have been at the center of scientific attention in the field of magnetism as a novel quantum state. The organic charge-transfer salt κ-(BEDT-TTF)$_2$Cu$_2$(CN)$_3$ (κ-CN), where BEDT-TTF is bis-(ethylenedithio)tetrathiafulvalene $C_6S_8[(CH_2)_2]_2$ (ET), has attracted attention in this area as a promising QSL candidate: the system is a weak dimer-Mott (DM) insulator forming a nearly isotropic two-dimensional triangular spin lattice which lacks long-range magnetic order down to low temperatures despite its large exchange coupling of $J \sim 250$ K [1]. Despite the absence of a magnetic phase transition, anomalous behavior at low temperatures around $T^* \sim 6$ K has been observed in various quantities probing either spin [1–6], charge [7], lattice [8–10], or composite properties thereof [11,12]; see also Ref. [13].

Recently, the discussion has taken a new twist from results of an electron spin resonance (ESR) study, reporting the formation of a spin-singlet state below about 6 K, consistent with a valence bond solid (VBS) ground state [4], but contradicting the QSL scenarios discussed so far. Arguments in favor of a glassy VBS state have been proposed by Riedl *et al.* [14] based on their analysis of magnetic data [6]. In addition to the signatures in the magnetic response, which are of moderate strength and prone to extrinsic factors [4], clear evidence for the strong involvement of the lattice in the 6 K anomaly was revealed by measurements of thermal expansion [9], ^{63}Cu NQR [8], and ultrasound velocity [10]. Since both the proposed QSL and VBS scenarios emerge through the 6 K anomaly, a clarification of its origin is key for understanding the ground state in this material.

Besides the spin and lattice degrees of freedom, indications for the presence of charge degrees of freedom within the dimers in κ-CN and various other related DM molecular conductors were pointed out. In κ-CN, a relaxor-type anomaly was observed in the dielectric constant below about 40 K, suggesting a charge disproportionation within the dimers and a freezing of these fluctuations on cooling towards 6 K [7,15,16]. As for the origin of these observations, conflicting results were reported based on measurements of charge-sensitive molecular vibrational modes. Whereas infrared optical spectroscopy failed to detect any clear line splitting, suggesting the absence of charge disproportionation [17], Raman scattering reveals a noticeable line broadening [18]. A similar relaxor-type dielectric behavior was observed for the DM insulator β'-(ET)$_2$ICl$_2$ [19], in which an intradimer charge disproportionation was reported. In addition, clear evidence for a first-order ferroelectric transition, accompanied by intradimer charge order [20], was revealed for κ-(ET)$_2$Hg(SCN)$_2$Cl [21]. Moreover, for the closely related DM system κ-(ET)$_2$Cu[N(CN)$_2$]Cl (κ-Cl), indications for long-range ferroelectric order coinciding with antiferromagnetic ordering below $T_N = 27$ K were observed [22,23].

*m_matsuura@cross.or.jp

In a recent inelastic neutron scattering (INS) study on this κ-Cl system it was found that the dynamics of a low-lying breathing/shearing mode of the ET dimers reacts sensitively to the charge and spin degrees of freedom once the π electrons become localized on the dimer site [24]. Motivated by these findings, we report here an INS study of low-energy intradimer vibrational modes on κ-CN for probing lattice effects and their coupling to charge and spin fluctuations associated with the 6 K anomaly.

Deuterated single crystals of κ-CN were grown by utilizing an electrochemical method [25]. The as-grown single crystals are thin plates (thickness of ~0.1 mm) with a flat and large crystal surface (a few mm^2) parallel to the bc plane (see Figs. S1(a) and (b) in the Supplemental Material (SM) [26]). Overall, forty-seven crystals (total mass of ~26 mg) were coaligned within 10 degrees in the $(0kl)$ scattering plane (Fig. S2 in SM [26]) according to their shape, i.e., the crystal edges including characteristic angles (Fig. S1(b) in SM [26]). The b and c axes were also confirmed using polarized micro infrared reflectance spectroscopy measurements for all the single crystals. In neutron scattering, the phonon scattering intensity is proportional to $(\boldsymbol{Q}\cdot\boldsymbol{\xi})^2$ where $\boldsymbol{Q}$ is the momentum transfer between the initial and final states of the neutron, and $\boldsymbol{\xi}$ is the polarization vector of the phonon mode. In order to detect the breathing mode of the ET dimers ($\boldsymbol{\xi} \parallel [011]$ or $[01\bar{1}]$), we measured phonon signals at $\boldsymbol{Q} = (060)$ [Figs. 1(f) and (g)]. INS experiments were performed using the triple-axis spectrometer IN8 at the Institut Laue Langevin [29]. The momentum transfers in this report are represented in units of reciprocal lattice vectors $b^* = 0.733$ Å^{-1} in the monoclinic notation. The initial and final neutron energies were selected using a doubly focused Cu (200) monochromator and analyzer, which resulted in an energy resolution of 0.62 meV at $\boldsymbol{Q} = (060)$ and $E = 0$. A pyrolytic graphite filter was placed in front of the analyzer to suppress higher-order neutrons.

Figure 1 shows the temperature dependence of the phonon spectra measured at $Q = (060)$ and $T = 1.5$–10 K. At $T = 1.5$ K, phonon peaks were observed at $E = 2.0$, 2.9, 3.7, 4.7, 5.7, and 7.2 meV, consistent with results of optical conductivity measurements on κ-CN [30]. According to density-functional-theory calculations [30], the peak at 4.7 meV can be assigned to an intradimer breathing mode. As the temperature rises, the intensity of this mode reduces, and all peaks become broad above 6 K. Since the linewidth of the peak is inversely proportional to the phonon lifetime, the broadening of these peaks indicates that the phonon lifetime becomes substantially reduced above 6 K.

The broadened phonon peaks were fitted using the damped harmonic-oscillator (DHO) function [31]:

$$\mathrm{DHO}_i(\boldsymbol{Q},\omega) = \frac{\Gamma_i\hbar\omega}{\left[\hbar^2\left(\omega^2-\omega_i^2\right)\right]^2+(\Gamma_i\hbar\omega)^2}, \qquad (1)$$

where Γ_i and $\hbar\omega_i$ denote the damping factor and phonon energy of the ith mode, respectively. The phonon spectra were fitted to a constant background and the sum of the DHO functions convolved with the resolution function $R(\boldsymbol{Q},\omega)$ using the RESTRAX simulation package [32]: $\sum_i \mathrm{DHO}_i(\boldsymbol{Q},\omega)\otimes R(\boldsymbol{Q},\omega)+BG$, where $\otimes$ denotes the convolution operator.

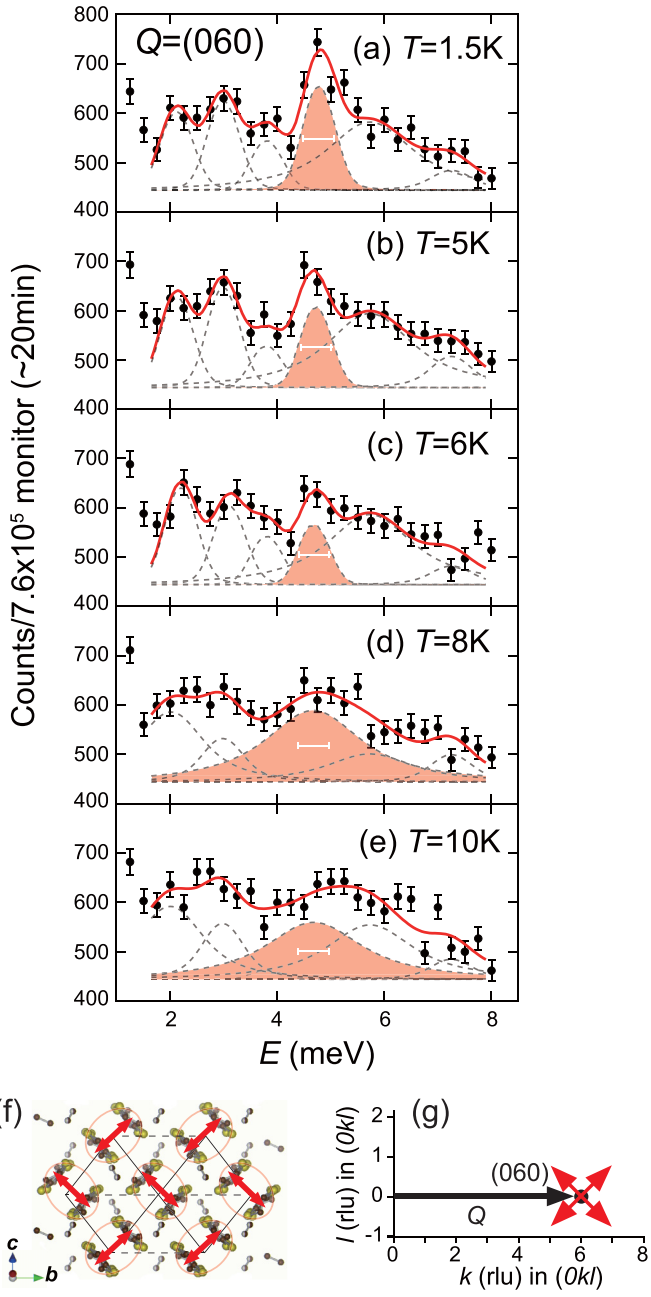

FIG. 1. (a)–(e) Temperature dependence of constant-Q scans at (060). The red curves are the sum of the fits to damped harmonic oscillator functions at $E \sim 2.0$, 2.9, 3.7, 4.7, 5.7, and 7.2 meV convolved with the experimental resolution. The dashed curves show the peak profiles for each mode. The breathing mode of the ET dimer at 4.7 meV is marked in red. The horizontal bars represent the instrumental energy resolution at $E = 4.7$ meV. (f) Top view of the ET layer. (g) Wave vector Q=(060) used for phonon measurements in the $(0kl)$ scattering plane. Red arrows in (f) and (g) show the polarization vector ξ of the breathing mode of the ET dimers, which can be detected at (060).

Figures 2(a)–2(c) show the temperature dependence of the DHO fitting parameters for the intradimer breathing mode. The peak energy remains constant within the error bars except for a slight hardening below $T^* \sim 6$ K [Fig. 2(a)]. Note

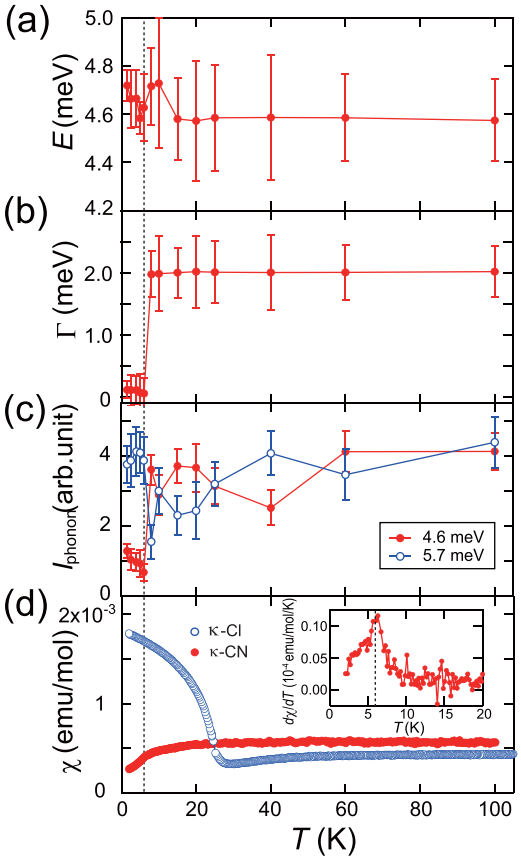

FIG. 2. Temperature dependence of (a) the phonon energy E and (b) the damping factor Γ of the breathing mode of ET dimers at $E \sim 4.7$ meV. (c) Thermal variation of the energy integrated intensity of the phonon modes ($I_{\rm phonon}$). (d) Temperature dependence of the uniform magnetic susceptibility χ measured on a single crystal in a magnetic field of 5 T perpendicular to the bc plane and for κ-Cl taken from Ref.[24]. Inset in (d) shows the temperature derivative of χ around the 6 K anomaly.

that a similar small change ($\Delta E \sim 0.2$ meV) in the phonon energy was observed also for the organic superconductor κ-$(ET)_2Cu(NCS)_2$ [33] upon cooling through the superconducting transition temperature, indicating a significant electron-phonon interaction in these soft organic compounds. The most prominent phonon anomaly in κ-CN is the change in the peak width at T^* as observed in the phonon spectra (Fig. 1) and the corresponding reduction in the damping factor Γ [Fig. 2(b)]. Whereas the large damping factor above T^* reflects an anharmonic lattice due to scattering processes, the small Γ below T^* suggests a freezing of these processes as the width becomes comparable to the instrumental resolution. In addition to the narrowing of the phonon linewidth for $T \leqslant T^*$, the integrated intensity ($I_{\rm phonon}$) of the breathing mode at $E = 4.7$ meV decreases significantly, whereas $I_{\rm phonon}$ is enhanced for the $E = 5.7$ meV mode [Fig. 2(c)]. The intensity of the mode at $E = 3.7$ meV also grows below T^* (Fig. 1). The disappearance of the $E = 3.7$ meV mode at $T = 8$ K and 10 K in Fig. 1 is probably due to small intensity close to the detection limit in the fitting. These changes in the phonon intensities at T^* indicate the transfer of spectral weight from the breathing modes to other vibration modes of the ET dimers.

For a deeper understanding of the scattering processes involved in the phonon renormalization effects revealed here for κ-CN, it is instructive to compare the results with those of the previously reported phonon study on the DM insulator κ-Cl. Despite some structural differences to κ-CN (Fig. S1 in SM [26]), in κ-Cl, a similar increase in the damping of a phonon peak at $E = 2.6$ meV was observed below $T_{\rm ins} \sim$ 50–60 K where the rapid increase in the resistivity reflects the opening of the charge gap [24]. These observations suggest a close coupling of low-energy intradimer breathing/shearing modes to the π electrons as a characteristic feature of these DM organic compounds.

In fact, following the phonon modes to higher temperature points to a correlation between the onset of phonon damping and the localization of the π electrons on the dimer sites, cf. Figs. S4 and S5 in SM [26]. Upon warming to $T = 100$ K, where κ-CN is still in its insulating, i.e., high-resistance DM state, the phonon modes remain broad. In contrast, for κ-Cl at this temperature, where the π electrons have regained a considerable degree of itineracy, as revealed in the resistivity, reflecting the closure of the charge gap, the spectrum exhibits well-defined phonon peaks (Figs. S4 and S5 in SM [26]).

These observations on κ-CN and κ-Cl suggest that it is the π electrons and their localization on the dimer site which cause the observed phonon damping. According to the pseudospin-coupling model [34], we expect the characteristic energy of the electrons' fluctuations in their charge or spin components to be of the same size as the energies of the low-lying optical phonon modes, i.e., $2-4$ meV. Once the fluctuations become frozen due to ordering in the charge and/or spin channel, the phonon lifetime recovers. In fact, such a reduction in Γ was observed for κ-Cl upon cooling below $T_{\rm N} = 27$ K [24] where magnetic order coinciding with ferroelectric order was observed [22].

Similar to κ-Cl, the bulk of experimental findings on κ-CN indicate fluctuations and ordering phenomena in both the charge- [7] and spin [4] sectors. A minimal model that describes the coupling between the spin and charge degrees of freedom within the dimers has been proposed based on the following Kugel-Khomskii-type Hamiltonian [15,16,35]:

$$\mathcal{H} = \sum_{\langle ij \rangle} J_{ij} \boldsymbol{S}_i \cdot \boldsymbol{S}_j - \sum_{\langle ij \rangle} V_{ij} Q_i^x Q_j^x + 2t_{\rm dim} \sum_i Q_i^z - \sum_{\langle ij \rangle} K_{ij} \boldsymbol{S}_i \cdot \boldsymbol{S}_j Q_i^x Q_j^x, \qquad (2)$$

where $\langle ij \rangle$ denotes the nearest-neighbor bonds; $\boldsymbol{S}_i$ and Q_i are the spin and charge pseudo-spin operators at the ith dimer unit, respectively. The x component in the pseudo-spin, $Q^x = \pm 1/2$, represents the polarized states of a hole on the dimer (cf. insets in Fig. 3), and the z component, $Q^z = 1/2(-1/2)$, represents a bonding (antibonding) state, where a hole is equally distributed on the two molecules. $J_{ij}(>0)$ is the interdimer exchange interaction, V_{ij} is the interdimer Coulomb interaction, $t_{\rm dim}$ (>0) is the intradimer hopping integral, and K_{ij} (>0) is the coupling between spins and dimer dipoles. Owing to the spin-charge coupling K_{ij}, the interaction between the neighboring Q^x is modulated by the spin-spin correlation as $V_{\rm eff} = V_{ij} + K \boldsymbol{S}_i \cdot \boldsymbol{S}_j$.

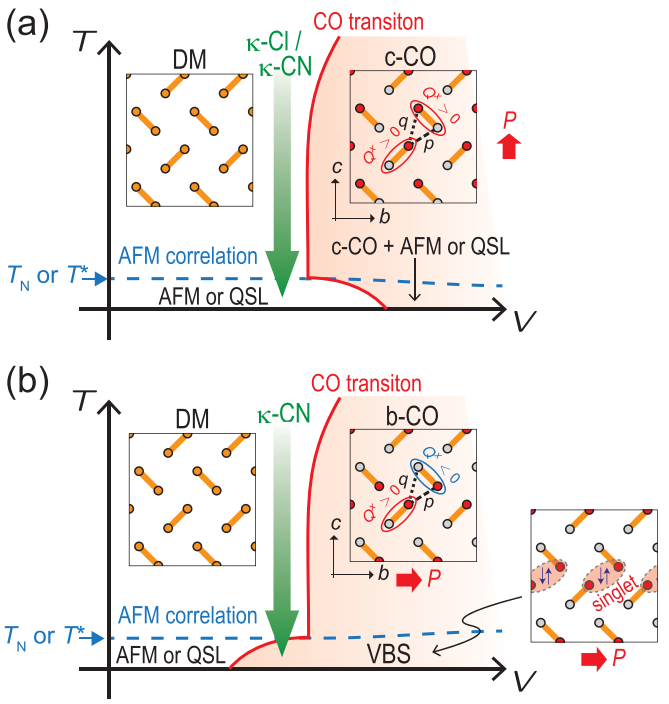

FIG. 3. Schematic phase diagrams of temperature (T) vs. interdimer Coulomb interaction (V) for (a) the QSL and (b) VBS states. The broken lines represent T_N for the case of κ-Cl whereas they correspond to a crossover for κ-CN. Insets: Spheres connected by thick orange lines represent ET dimers. White and red spheres correspond to charge-poor and charge-rich sites, respectively.

Figure 3 shows schematic phase diagrams in the V-T plane, deduced using the mean-field analysis of Eq. (2) [35] where the DM ($\langle Q^x \rangle = 0$) and charge order (CO) ($\langle Q^x \rangle > 0$) phases compete. In DM insulators, two patterns of CO are possible: b-CO and c-CO types, in which polarization occurs along the b and c axes, respectively. The direction of the electric polarization strongly depends on the sign of $V_{ij} = V_p - V_q$ on the diagonal bonds, termed p and q in Fig. 3. In several κ-type ET compounds, $V_p > V_q$ is obtained assuming a $1/r$-type dependence of V_{ij}, which prefers the c-CO state [15,16,36]. However, since the magnitudes of V_p and V_q are almost identical, it is quite possible that other effects, e.g., due to electron-lattice coupling, make the V_{ij} effectively negative, resulting in the b-CO state. When AFM correlations develop ($\boldsymbol{S}_i \cdot \boldsymbol{S}_j < 0$), $|V_{\rm eff}|$ becomes smaller for the c-CO ($V_{ij} > 0$), whereas $|V_{\rm eff}|$ is enhanced for the b-CO ($V_{ij} < 0$). Thus, due to the effects of AFM correlations, the c-CO is suppressed [Fig. 3(a)], while the b-CO is enhanced [Fig. 3(b)], resulting in a VBS phase, i.e., a spin-singlet state. Therefore, depending on the type of CO, different V-T phase diagrams are obtained below T^*.

In what follows, we discuss our experimental findings on phonon damping and its suppression below $T^* \sim 6$ K for the two scenarios shown in Fig. 3. In the QSL scenario (c-CO) [Fig. 3(a)], these charge fluctuations become harder at low temperatures, resulting in a decoupling between the lattice and charge degrees of freedom. For the VBS scenario (b-CO) [Fig. 3(b)], spin singlets form via a spin-Peierls-like transition at T^*. In this case, a spin gap is opening and a hardening of charge fluctuations is expected as well. Thus, a phonon anomaly at T^* is expected through the decoupling of the lattice degrees of freedom from either the charge or the charge and spin degrees of freedom, corresponding to the QSL or VBS scenarios, respectively. Then, the key difference between these scenarios is whether the system undergoes a distinct phase transition at T^* [Fig. 3(b)] or a crossover [Fig. 3(a)]. The present finding of an abrupt change in the phonon linewidths at T^* is considered a strong indication for a phase transition, supporting the VBS scenario.

Several experimental [7,38] and theoretical [15,37] observations suggest that κ-CN is located near the DM/CO phase boundary for temperatures above T^*, cf. Fig. 3. Upon cooling κ-CN comes closer to the CO phase boundary, corresponding to a softening of the intradimer charge fluctuations [37] (see Fig. S6 in SM [26]). This is consistent with the growth of charge fluctuations observed in the optical conductivity upon cooling towards T^* [38]. The distinct c-axis polarization of the fluctuations revealed in these experiments would be in support of the QSL scenario. On the other hand, arguments in favor of a VBS scenario can be derived from the observation of a spin gap [4,13] in combination with findings from thermal expansion measurements where well-pronounced signatures were observed at T^* [9,39]. In particular, these latter data provide strong evidence for a second-order phase transition at $T^* \sim 6$ K, rather than a crossover, albeit with significant sample-to-sample variations in the shape of the anomaly [39]. Moreover, for those crystals where the effects are most strongly pronounced, the phase transition anomaly shows striking similarities to that revealed for the spin-Peierls transition in $(TMTTF)_2AsF_6$ [40]. A phase transition into a VBS state, suggested by these results, would also be consistent with the abrupt change in the phonon linewidth, and the sharp feature observed in $d\chi/dT$ at T^* [cf. inset of Fig. 2(d)].

In conclusion, by studying the spectra of selected low-energy optical phonons of the quantum spin liquid candidate κ-$(ET)_2Cu_2(CN)_3$ as a function of temperature, we observe an abrupt change in the phonon linewidth at $T^* \sim 6$ K. We argue that the recovery of long-lived (underdamped) breathing modes of ET-dimers below 6 K can be attributed to a cooperative phenomenon involving the lattice and its coupling to the charge and spin degrees of freedom around 6 K. Our data are consistent with the formation of a VBS state below 6 K.

We thank N. Sato and S. Sugiura for their help in preparating the experiments. The neutron experiments were performed with the approval of ILL (7-01-513) [41]. This study was financially supported by Grants-in-Aid for Scientific Research (19H01833, 19K03723, 20H05144, and 22H04459) from the Japan Society for the Promotion of Science. This work was partly performed under the GIMRT Program of the Institute for Materials Research, Tohoku University (Proposals No. 202111-RDKGE-0004, No. 202112-RDKGE-0019, and No. 202012-RDKGE-0042). Work at Goethe University, Frankfurt, was supported by the Deutsche Forschungsgemeinschaft (DFG, German Science Foundation) for funding through TRR 288-422213477 (Project A06 and B02).

[1] Y. Shimizu, K. Miyagawa, K. Kanoda, M. Maesato, and G. Saito, Spin Liquid State in an Organic Mott Insulator with a Triangular Lattice, Phys. Rev. Lett. **91**, 107001 (2003).

[2] F. Pratt, P. Baker, S. Blundell, T. Lancaster, S. Ohira-Kawamura, C. Baines, Y. Shimizu, K. Kanoda, I. Watanabe, and G. Saito, Magnetic and non-magnetic phases of a quantum spin liquid, Nature (London) **471**, 612 (2011).

[3] Y. Shimizu, K. Miyagawa, K. Kanoda, M. Maesato, and G. Saito, Emergence of inhomogeneous moments from spin liquid in the triangular-lattice Mott insulator κ-$(ET)_2Cu_2(CN)_3$, Phys. Rev. B **73**, 140407(R) (2006).

[4] B. Miksch, A. Pustogow, M. J. Rahim, A. A. Bardin, K. Kanoda, J. A. Schlueter, R. Hübner, M. Scheffler, and M. Dressel, Gapped magnetic ground state in quantum spin liquid candidate κ-$(BEDT\text{-}TTF)_2Cu_2(CN)_3$, Science **372**, 276 (2021).

[5] Y. Saito, T. Minamidate, A. Kawamoto, N. Matsunaga, and K. Nomura, Site-specific ^{13}C NMR study on the locally distorted triangular lattice of the organic conductor κ-$(BEDT\text{-}TTF)_2Cu_2(CN)_3$, Phys. Rev. B **98**, 205141 (2018).

[6] T. Isono, T. Terashima, K. Miyagawa, K. Kanoda, and S. Uji, Quantum criticality in an organic spin-liquid insulator κ-$(BEDT\text{-}TTF)_2Cu_2(CN)_3$, Nat. Commun. **7**, 13494 (2016).

[7] M. Abdel-Jawad, I. Terasaki, T. Sasaki, N. Yoneyama, N. Kobayashi, Y. Uesu, and C. Hotta, Anomalous dielectric response in the dimer Mott insulator κ-$(BEDT\text{-}TTF)_2Cu_2(CN)_3$, Phys. Rev. B **82**, 125119 (2010).

[8] T. Kobayashi, Q.-P. Ding, H. Taniguchi, K. Satoh, A. Kawamoto, and Y. Furukawa, Charge disproportionation in the spin-liquid candidate κ-$(ET)_2Cu_2(CN)_3$ at 6 K revealed by ^{63}Cu NQR measurements, Phys. Rev. Res. **2**, 042023(R) (2020).

[9] R. S. Manna, M. de Souza, A. Brühl, J. A. Schlueter, and M. Lang, Lattice Effects and Entropy Release at the Low-Temperature Phase Transition in the Spin-Liquid Candidate κ-$(BEDT\text{-}TTF)_2Cu_2(CN)_3$, Phys. Rev. Lett. **104**, 016403 (2010).

[10] M. Poirier, M. de Lafontaine, K. Miyagawa, K. Kanoda, and Y. Shimizu, Ultrasonic investigation of the transition at 6 K in the spin-liquid candidate κ-$(BEDT\text{-}TTF)_2Cu_2(CN)_3$, Phys. Rev. B **89**, 045138 (2014).

[11] S. Yamashita, Y. Nakazawa, M. Oguni, Y. Oshima, H. Nojiri, Y. Shimizu, K. Miyagawa, and K. Kanoda, Thermodynamic properties of a spin-1/2 spin-liquid state in a κ-type organic salt, Nat. Phys. **4**, 459 (2008).

[12] M. Yamashita, N. Nakata, Y. Kasahara, T. Sasaki, N. Yoneyama, N. Kobayashi, S. Fujimoto, T. Shibauchi, and Y. Matsuda, Thermal-transport measurements in a quantum spin-liquid state of the frustrated triangular magnet κ-$(BEDT\text{-}TTF)_2Cu_2(CN)_3$, Nat. Phys. **5**, 44 (2009).

[13] A. Pustogow, Thirty-year anniversary of κ-$(BEDT\text{-}TTF)_2Cu_2(CN)_3$: Reconciling the spin gap in a spin-liquid candidate, Solids **3**, 93 (2022).

[14] K. Riedl, R. Valentí, and S. M. Winter, Critical spin liquid versus valence-bond glass in a triangular-lattice organic antiferromagnet, Nat. Commun. **10**, 2561 (2019).

[15] M. Naka and S. Ishihara, Electronic ferroelectricity in a dimer Mott insulator, J. Phys. Soc. Jpn. **79**, 063707 (2010).

[16] C. Hotta, Quantum electric dipoles in spin-liquid dimer Mott insulator κ-$ET_2Cu_2(CN)_3$, Phys. Rev. B **82**, 241104(R) (2010).

[17] K. Sedlmeier, S. Elsässer, D. Neubauer, R. Beyer, D. Wu, T. Ivek, S. Tomić, J. A. Schlueter, and M. Dressel, Absence of charge order in the dimerized k-phase BEDT-TTF salts, Phys. Rev. B **86**, 245103 (2012).

[18] K. Yakushi, K. Yamamoto, T. Yamamoto, Y. Saito, and A. Kawamoto, Raman spectroscopy study of charge fluctuation in the spin-liquid candidate κ-$(BEDT\text{-}TTF)_2Cu_2(CN)_3$, J. Phys. Soc. Jpn. **84**, 084711 (2015).

[19] S. Iguchi, S. Sasaki, N. Yoneyama, H. Taniguchi, T. Nishizaki, and T. Sasaki, Relaxor ferroelectricity induced by electron correlations in a molecular dimer Mott insulator, Phys. Rev. B **87**, 075107 (2013).

[20] N. Drichko, R. Beyer, E. Rose, M. Dressel, J. A. Schlueter, S. A. Turunova, E. I. Zhilyaeva, and R. N. Lyubovskaya, Metallic state and charge-order metal-insulator transition in the quasi-two-dimensional conductor κ-$(BEDT\text{-}TTF)_2Hg(SCN)_2Cl$, Phys. Rev. B **89**, 075133 (2014).

[21] E. Gati, J. K. H. Fischer, P. Lunkenheimer, D. Zielke, S. Köhler, F. Kolb, H. A. K. von Nidda, S. M. Winter, H. Schubert, J. A. Schlueter, H. O. Jeschke, R. Valenti, and M. Lang, Evidence for Electronically Driven Ferroelectricity in a Strongly Correlated Dimerized BEDT-TTF Molecular Conductor, Phys. Rev. Lett. **120**, 247601 (2018).

[22] P. Lunkenheimer, J. Müller, S. Krohns, F. Schrettle, A. Loidl, B. Hartmann, R. Rommel, M. de Souza, C. Hotta, J. A. Schlueter, Multiferroicity in an organic charge-transfer salt that is suggestive of electric-dipole-driven magnetism *et al.*, Nat. Mater. **11**, 755 (2012).

[23] M. Lang, P. Lunkenheimer, J. Müller, A. Loidl, B. Hartmann, N. H. Hoang, E. Gati, H. Schubert, and J. A. Schlueter, Multiferroicity in the Mott Insulating Charge-Transfer Salt κ-$(BEDT\text{-}TTF)_2Cu[N(CN)_2]Cl$, IEEE Trans. Magn. **50**, 2700107 (2014).

[24] M. Matsuura, T. Sasaki, S. Iguchi, E. Gati, J. Müller, O. Stockert, A. Piovano, M. Böhm, J. T. Park, S. Biswas, S. M. Winter, R. Valentí, A. Nakao, and M. Lang, Inelastic Neutron Scattering Measurements on the Molecular Dimer-Mott Insulator κ-$(BEDT\text{-}TTF)_2Cu[N(CN)_2]Cl$, Phys. Rev. Lett. **123**, 027601 (2019).

[25] U. Geiser, H. H. Wang, K. D. Carlson, J. M. Williams, H. A. Charlier Jr, J. E. Heindl, G. A. Yaconi, B. J. Love, and M. W. Lathrop, Superconductivity at 2.8 K and 1.5 kbar in κ-$(BEDT\text{-}TTF)_2Cu_2(CN)_3$: The first organic superconductor containing a polymeric copper cyanide anion, Inorg. Chem. **30**, 2586 (1991).

[26] See Supplemental Material at http://link.aps.org/supplemental/10.1103/PhysRevResearch.4.L042047 for the details of the photo and the crystal structure of κ-CN, rocking curves, temperature dependence of constant-Q scans at (060), phonon spectra at $T = 100$ K for κ-CN and κ-Cl, temperature dependence of the electric resistivity, and schematic diagram of the temperature dependence of the charge fluctuations and coupled phonon frequency, which includes Refs. [27,28].

[27] U. Geiser, A. J. Schults, H. H. Wang, D. M. Watkins, D. L. Stupka, J. M. Williams, J. Schirber, D. Overmyer, D. Jung, J. Novoa, and M.-H. Whangbo, Strain index, lattice softness and superconductivity of organic donor-molecule salts: Crystal and electronic structures of three isostructural salts κ-$(BEDT\text{-}TTF)_2Cu[N(CN)_2]X$ (X =Cl, Br, I), Physica C **174**, 475 (1991).

[28] K. Momma and F. Izumi, VESTA3 for three-dimensional visualization of crystal, volumetric and morphology data, J. Appl. Crystallogr. **44**, 1272 (2011).

[29] A. Hiess, M. Jiménez-Ruiz, P. Courtois, R. Currat, J. Kulda, and F. J. Bermejo, ILL's renewed thermal three-axis spectrometer IN8: A review of its first three years on duty, Phys. B: Condens. Matter **385**, 1077 (2006).

[30] M. Dressel, P. Lazić, A. Pustogow, E. Zhukova, B. Gorshunov, J. A. Schlueter, O. Milat, B. Gumhalter, and S. Tomić, Lattice vibrations of the charge-transfer salt κ-(BEDT-TTF)$_2$Cu$_2$(CN)$_3$: Comprehensive explanation of the electrodynamic response in a spin-liquid compound, Phys. Rev. B **93**, 081201(R) (2016).

[31] K. Gesi, J. D. Axe, G. Shirane, and A. Linz, Dispersion and Damping of Soft Zone-Boundary Phonons in $KMnF_3$, Phys. Rev. B **5**, 1933 (1972).

[32] J. Saroun and J. Kulda, RESTRAX - program for TAS resolution calculation and scan profile simulation, Phys. B: Condens. Matter **234**, 1102 (1997).

[33] L. Pintschovius, H. Rietschel, T. Sasaki, H. Mori, S. Tanaka, N. Toyota, M. Lang, and F. Steglich, Observation of superconductivity-induced phonon frequency changes in the organic superconductor κ-(BEDT-TTF)$_2$Cu(NCS)$_2$, Europhys. Lett. **37**, 627 (1997).

[34] Y. Yamada, H. Takatera, and D. L. Huber, Critical dynamical phenomena in pseudospin-phonon coupled systems, J. Phys. Soc. Jpn. **36**, 641 (1974).

[35] M. Naka and S. Ishihara, Magnetoelectric effect in organic molecular solids, Sci. Rep. **6**, 20781 (2016).

[36] H. Watanabe, H. Seo, and S. Yunoki, Mechanism of superconductivity and electron-hole doping asymmetry in κ-type molecular conductors, Nat. Commun. **10**, 1 (2019).

[37] M. Naka and S. Ishihara, Collective charge excitation in a dimer Mott insulating system, J. Phys. Soc. Jpn. **82**, 023701 (2013).

[38] K. Itoh, H. Itoh, M. Naka, S. Saito, I. Hosako, N. Yoneyama, S. Ishihara, T. Sasaki, and S. Iwai, Collective Excitation of an Electric Dipole on a Molecular Dimer in an Organic Dimer-Mott Insulator, Phys. Rev. Lett. **110**, 106401 (2013).

[39] R. S. Manna, S. Hartmann, E. Gati, J. A. Schlueter, M. De Souza, and M. Lang, Low-temperature Lattice Effects in the Spin-Liquid Candidate κ-(BEDT-TTF)$_2$Cu$_2$(CN)$_3$, Crystals **8**, 87 (2018).

[40] M. de Souza, A. Brühl, J. Müller, P. Foury-Leylekian, A. Moradpour, J.-P. Pouget, and M. Lang, Thermodynamic studies at the charge-ordering and spin-Peierls transitions in (TMTTF)$_2$X, Phys. B: Condens. Matter **404**, 494 (2009).

[41] M. Matsuura, M. Lang, J. Müller, A. Piovano, T. Sasaki, O. Stockert, and R. Valenti, Study of lattice contribution to the quantum spin liquid properties in molecular dimer-Mott insulator κ-(BEDT-TTF)$_2$Cu$_2$(CN)$_3$ (Institut Laue-Langevin (ILL), Grenoble, 2021), doi: 10.5291/ILL-DATA.7-01-513.